Article

Not peer-reviewed version

Characteristics and Mechanism of the Ore-Forming Fluids in the Shimensi Tungsten Polymetallic Deposit in Southeastern China

Peng Wang , Zhanghuang Ye * , Xiaohua Zong

Posted Date: 7 May 2024

doi: 10.20944/preprints202405.0369.v1

Keywords: fluid inclusions; H-O isotope; Shimensi tungsten deposit

Article

Characteristics and Mechanism of the Ore-Forming Fluids in the Shimensi Tungsten Polymetallic Deposit in Southeastern China

Peng Wang [1,2], Zhanghuang Ye [3] and Xiaohua Zong [2]**

[1] School of Earth Science and Resources, Chang'an University, Xi'an, 710054, Shaanxi, China
[2] Sino Shaanxi Nuclear Industry Group 214 Brigade Co.Ltd, Xi'an, 710054, Shaanxi, China
[3] Jiangxi Science and Technology Normal University, Nanchang, 330038, Jiangxi, China
* Correspondence: chuckverna@sina.com

Abstract: The Shimensi super-large tungsten polymetallic deposit is located in Late Jurassic- Early Cretaceous Porphyry-Skarn tungsten ore belt in the south Yangtze metallogenic belt. There are 3 types of mineralization: veinlet-disseminated type, thick quartze vein type and hydrothermal crypto-explosive breccia type. Based on geological studies, this paper presents new petrographic, microthermometric, laser Raman spectroscopic and hydrogen and oxygen isotope research of the fluid inclusions from the deposit. The results show that there are five different types of fluid inclusions: liquid-rich inclusions, vapor-rich inclusions, pure liquid inclusions, pure vapor inclusions, and fluid inclusions containing a solid crystal. The homogenization temperatures of the fluid inclusion range from 140℃-270℃, the salinities are 3%-5% $NaCl_{eq}$ and the densities of ore-forming fluid range from 0.64 g/cm^3 to 0.99 g/cm^3. For the analyses of Laser Raman spectroscopic, the ore-forming fluids can be approximated by a Ca^{2+}-Na^{+}-SO_4^{2-}-Cl^{-} fluid system with small amount of CO_2, CH_4 and N_2. Otherwise, the datas of the pressure, pH and Eh show a fluid metallogenic environment of low pressure, weak acid and weak reduction. The values of the homogenization temperature in 3 types of orebodies suggest that the mineralization is characterized by the decrease of the temperature under the condition of the fluid immiscibility. The H-O isotope values are interpreted to indicate that the ore-forming fluids are mainly composed of magmatic water, and also the meteoric water was added with the process of the magma rising.

Keywords: fluid inclusions; H-O isotope; Shimensi tungsten deposit

1. Introduction

Jiangxi Province is an important W producer in China and hosts several giant tungsten deposits in its southern region, such as Xihuashan and Dajishan [1–4]. With the development of the geological prospecting , a cluster of world class W deposits have been discovered in the northern Jiangxi province, including the Dahutang W-Cu-Mo, Xianglushan W, Yangchuling W-Mo, and Zhuxi W-Cu-Mo deposits [5]. The discovery of these tungstern polymetallic deposits has gradually changed the distribution patterns of Jiangxi province, and even in China.

The Dahutang super-large tungsten polymetallic ore field is located in the Late Jurassic-Early Cretaceous porphyry-skarn tungsten ore zone of the Jiangnan Orogen between the Yangtze and Cathaysia Craton [6,7]. The Dahutang ore field has an estimated reserves of 2 million tons of WO_3@0.152%W, accompanied by 500 Kt Cu@0.12%Cu and 80.2 Kt Mo@0.098%Mo [8]. The discovery of the Dahutang polymetallic ore district, especially the veinlet-disseminated scheelite mineralization in the biotite granodorite of the Shimensi deposit, has changed the exploration strategy of focusing on the quartz vein type wolframite mineralization [9].

The Shimensi tungsten deposit itself is situated at the junction of Wuning, Xiushui and Jing'an Counties in the north of the Dahutang ore field. By May 2012, the 916 Corps of Jiangxi Bureau of

 doi:10.20944/preprints202405.0369.v1

Geological Exploration for Mining Resources has invested 77 drills, completed a drilling footage of 190 kilometers, and submitted 743,000 tons of WO_3 resources with an average grade of 0.195%, accompanied by 4000 Kt Cu and 28 Kt Mo [10]. Although the Shimensi tungsten deposit has been studies extensively in recent years, most of them have focused on the geological characteristics, metallogenic chronology, mineralization background, ore-forming material sources, etc [11–25], little is known about the characteristics of ore-forming fluids and their geneses in the region. Based on previous results, this paper examines fluid inclusions in three main types of ore bodies in the area in detail, and discusses the characteristics and sources of ore-forming fluids. This provides a new geochemical basis for studying the widespread enrichment of tungsten in the Shimensi tungsten deposit.

2. Regional Geological Background

Since the Mesoproterozoic era, the Jiangnan orogenic belt has long been under the control of the Yangtze Plate and Cathaysia Plates and their junction zones [26,27]. After undergoing magmatic-sedimentary-metamorphic-tectonic-metallogenic events as well the Indosinian tectonic movement, the belt was transformed to a continent. During the Yanshanian Tectonic Movement, due to intraplate contraction and the interaction of the Kula-Pacific Ocean Plates with the neighboring plates, strong continental orogeny occurred in the region, and brought about an NE-NEE-dominated strike slip thrust extensional structure [28,29], which was superimposed and compounded with the ancient structure, bringing up rich nonferrous, rare and precious metal minerals(Figure 1).

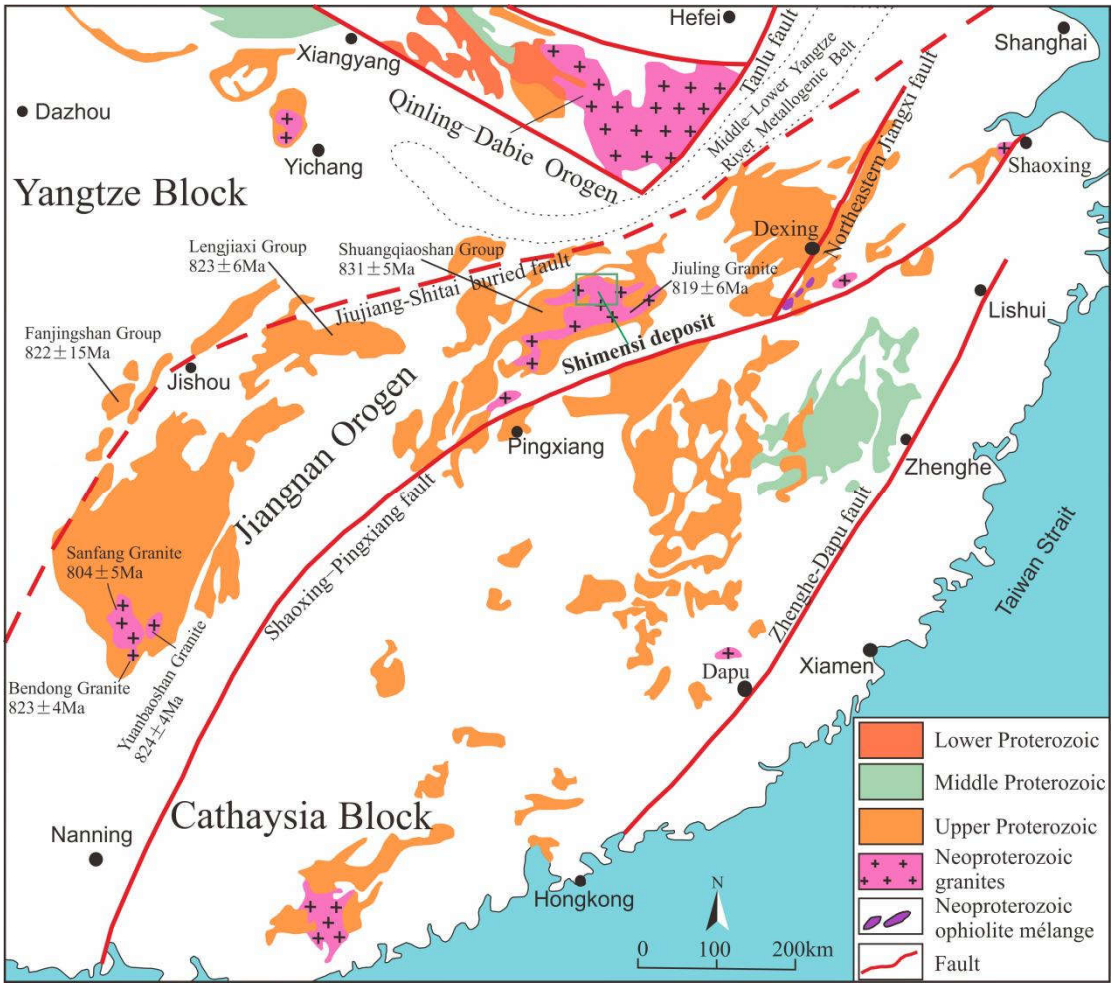

Figure 1. Map presenting the distribution of granites and volcanic rocks in south China, and also the location of the Jiangnan Orogen and the Shimensi ore deposit (modified after [25]).

Preprints.org (www.preprints.org) | NOT PEER-REVIEWED | Posted: 7 May 2024 doi:10.20944/preprints202405.0369.v1

The exposed strata of Dahutang ore field are mainly the Mesoproterozoic shallow metamorphic rock series of Anlelin Formation of Shuangqiaoshan Group, with intermediate basic ancient volcanic rock layers inside, which is one of the important metallogenic wall rocks in the area. The fracturing structures in the area are mainly near EW and NE-NNE trending, followed by NW and NS trending. Near EW trending fractures are mainly distributed on the north and south of the ore field, represented by the northern Luositang-Xin'anli fracture, which extends for more than several kilometers and is manifested as strong silicification zone and compression fracture zone. The NE-NNE trending fractures are the most developed within the region and run through the whole area, represented by the NNE trending strike slip thrust belt extensional structure of Wuning-Yifeng-Lianhuashan, which is dominated by compression and torsion. NW trending fractures are not widely distributed in the area, with two relatively larger faults distributed in Guanyintang-Maogongdong-Shimensi areas.

A large area of intermediate-acid/acid rock is exposed in the area, mainly composed of Jinning stage medium coarse biotite granodiorite, which occurs as a batholith. There are two tectonic magmatic rock belts in Yanshanian rock mass, of which the Huangshaqiao-Meimaoshan magmatic rock belt in the west is the early Yanshanian monzonite, occurring as a batholith, with a total exposed area of more than 100 km². Dozens of rock bodies (veins) are distributed in the eastern Jiulongjian Dahutang tectonic magmatic rock belt. From the north to the south, there are five rock bodies: Xin'anli, Shimensi, Dahutang, Shiweidong and Jiulongjian, with an area of 0.3~3 km². Only a small part of the three rock bodies (Shimensi, Dahutang and Shiweidong) are exposed to the surface while most of them are hidden below. The rock body in the shape of a rock stem was formed in the early Yanshanian period. Its zircon U-Pb isotopic age is 136～138 Ma [14]. Its lithology is mainly porphyritic biotite granite, fine biotite granite and granite porphyry. It is closely related to the mineralization of tungsten, tin and molybdenum. From north to south, it is manifested as W-Sn-Mo-Cu-Ag (Dahutang ore concentration area) → Mo-W-Cu (Yangshidian) → Cu-Mo-W (Jiulongjian) mineralization zoning(Figure 2).

The main deposit types are quartz vein - fine vein disseminated altered granite-composite deposit type (Shiweidong), quartz vein- fine vein disseminated cryptoexplosive breccia altered granite- composite deposit (Shimensi, Dalingshang), fine vein disseminated altered granite greisen - composite deposit (Dongdouya), quartz vein belt type (Yangshidian), fine vein disseminated altered granite blasting breccia composite deposit (Shiziyan) and tectonic altered rock type (Jiulongjian). All are post magmatic hydrothermal deposits related to Yanshanian rock mass.

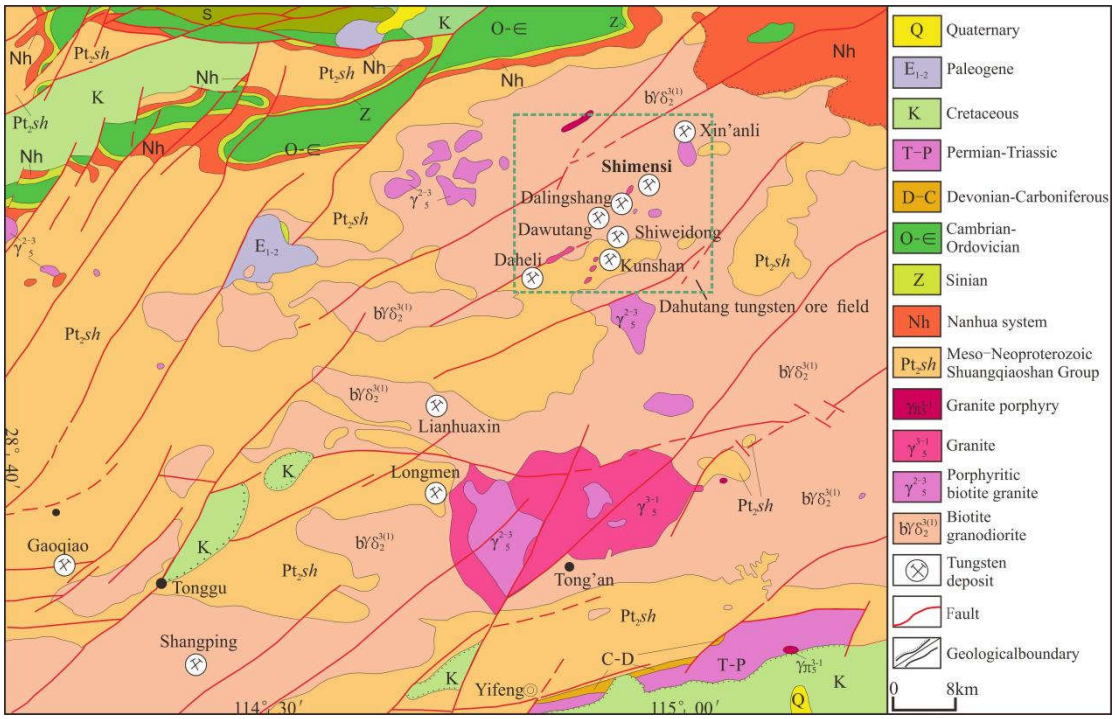

 doi:10.20944/preprints202405.0369.v1

Figure 2. Geological and mineral map of the Jiulingshan region.

3. Deposit Geology

The Shimensi tungsten deposit has experienced multiple periods and stages of magmatic activity. The biotite granodiorite formed in the late Jinning period is a part of Jiuling batholith. The porphyritic biotite granite(with porphyritic texture, coarse grained phenocrysts, medium fine grained matrix), fine grained biotite granite, and biotite granite porphyry(with porphyritic texture, medium fine phenocrysts and aphanitic matrix), which successively intruded in the middle Yanshan period, have a regularly-refined particle size. It shows that their formation depth becomes shallower and their invasion time later in turn [30]. The Yanshanian porphyritic biotite granite is a W-Cu ore-forming rock body, while Jinningian biotite granodiorite is the main ore hosting body (Figure 3).

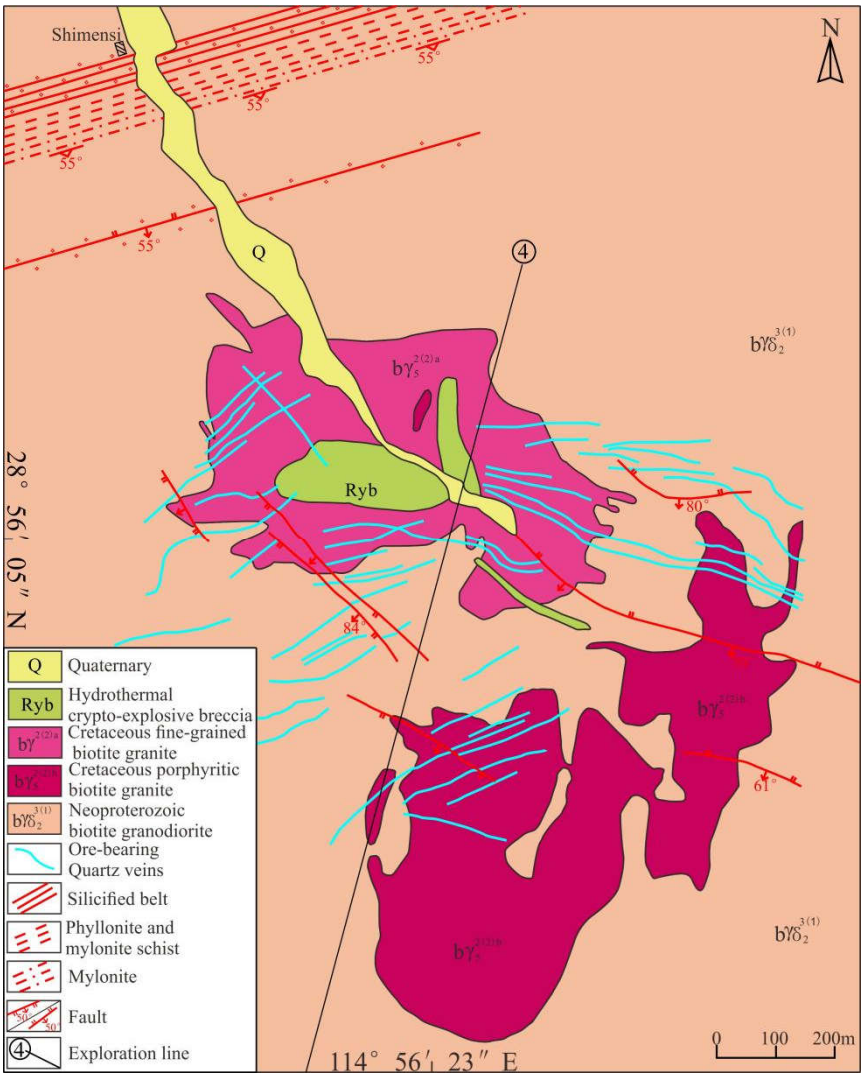

Figure 3. Geological map of the Shimensi deposit.

The structure of the ore field is mainly manifested in three ways, namely, ductile shear zone, fracture and joint. According to the strike, it can be divided into four groups: NNE, NEE, NE and NW, with NW trending fractures most developed [30].

The formation of Shimensi deposit takes Yanshanian plutonic to hypabyssal granite body as the metallogenic parent rock, and its genetic type is post magmatic medium low temperature deposit. The industrial types of ores can be divided into veinlet disseminated type, crypto explosive breccia type and quartz vein type, which are characterized by multiple mineralization and “one field, three types” [30].

Preprints.org (www.preprints.org) | NOT PEER-REVIEWED | Posted: 7 May 2024 doi:10.20944/preprints202405.0369.v1

The vein disseminated ore bodies are distributed in the main sections of Shimensi deposit, and occur in the inner and outer contact zones of porphyritic biotite granite in Mid-Yanshanian Period and biotite granodiorite batholith in the Late-Jinning Period. The mode of occurrence is generally gentle, basically consistent with the mode of occurrence of the contact surface, and tends to change with the contact surface (Figure 4). Among them, thick industrial tungsten (copper) ore bodies can be seen in the outer contact zone with a good mineralization continuity. The ore bodies in the inner contact zone are generally thin and poor, with many inclusions and poor mineralization continuity. The alteration type is closely related to the lithology of wall rock. The K-feldsparization in porphyritic biotite granite in the inner contact zone is more obvious, and the biotite granodiorite in the outer contact zone is more obvious. The common alteration of the two is greisenization and chloritization. The crypto explosive breccia type ore bodies are mainly distributed in the middle of Shimensi ore field. The crypt explosive breccia is developed in the middle Yanshanian fine-grained biotite granite and granite porphyry penetrated along the F20 fracture, mainly in breccia and net vein mineralization. The ore body minerals are various and the ore mineral combination is complex, mainly including wolframite, scheelite, chalcopyrite, molybdenite, etc. The quartz vein type ore bodies are mainly distributed in the range of about 0.6 km² in the middle of the ore district, cutting through all rock units and other types of ore bodies in the ore district.

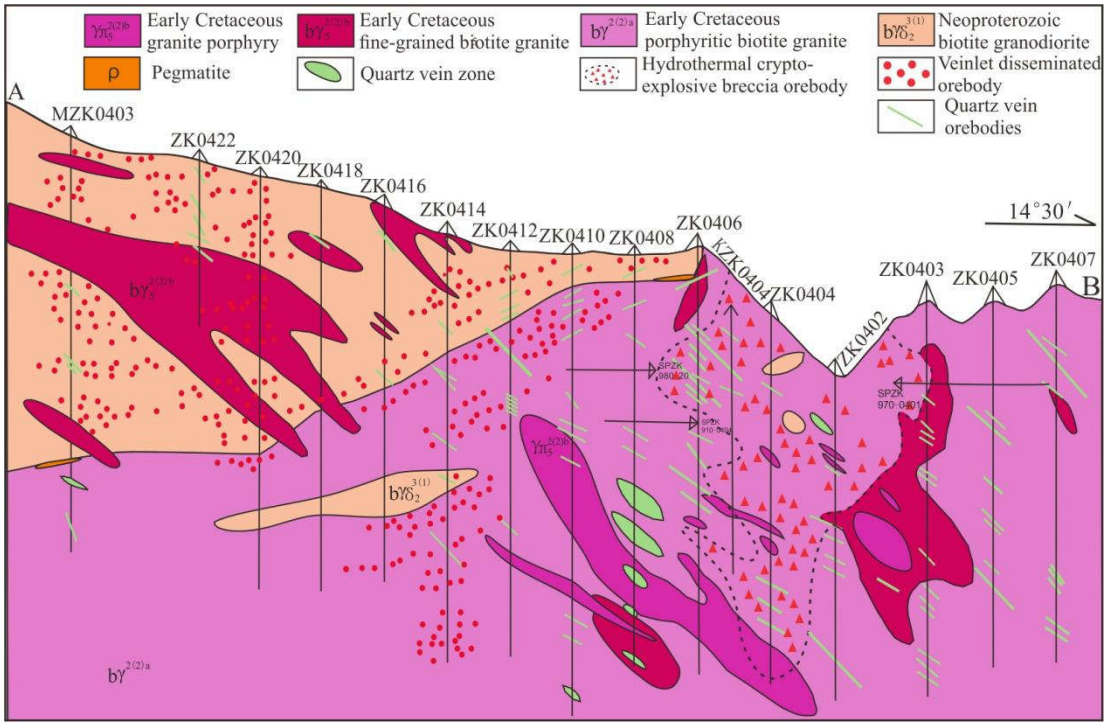

Figure 4. Geological map of the Shimensi No. 4 prospecting line, showing the three ore types: veinlet-disseminated, hydrothermal crypto-explosive breccia and quartz veins.

4. Sampling and Analytical Methods

Three types of ore bodies are basically covered by the samples in this study. Samples are collected from different elevations, drills and tunnels (Table 1). A total of 26 inclusion slices were milled, and the inclusions of quartz in various types of ore bodies were studied in detail. Single minerals were selected for fluid inclusion composition and H-O isotope test.

 doi:10.20944/preprints202405.0369.v1

Table 1. Characteristics and locations of samples for microthermometric studies of the Shimensi tungsten deposit.

Sample	Ore body type	Location	mineralogy
SM001	thick quartz vein type	No.402 mine, 45m	wolframite, chalcopyrite, molybdenite, scheelite
SM002		ZK1201, 55m	chalcopyrite and scheelite
SM009		No.2 mine, 38m	wolframite, chalcopyrite, molybdenite, scheelite
SM010		No.2 mine ,YM2, 2m	chalcopyrite, molybdenite, scheelite
SM013		No.2 mine, YM2, 35m	chalcopyrite, molybdenite
SM033		No.401mine, tunnel openings	wolframite, chalcopyrite, molybdenite
SM034		No.401 mine ,YM1, 3m	wolframite, chalcopyrite, molybdenite, scheelite
SM035		No.801mine, 30m	wolframite, chalcopyrite, molybdenite, scheelite
SM037		No.802 mine ,40m	wolframite, chalcopyrite, molybdenite, scheelite
SM003	hydrothermal crypto-explosive breccia type	No.402 mine, tunnel openings	wolframite, chalcopyrite, molybdenite, scheelite
SM006		No.3 mine, 15m	wolframite, chalcopyrite, molybdenite, scheelite
SM008		inclined shaft,120m	wolframite, chalcopyrite, molybdenite, scheelite
SM036		No.802 mine, H134	chalcopyrite, molybdenite, scheelite
SM038		No.802 mine, H30	chalcopyrite, molybdenite, scheelite
SM056	veinlet-disseminated type	ZK0408, 156m	greisenization and veinlet-disseminated scheelite on both sides of quartz vein
SM021		KZK0801, 396m	greisenization and veinlet-disseminated scheelite on both sides of quartz vein
SM024		ZK0803, 92m	greisenization and veinlet-disseminated scheelite on both sides of quartz vein
SM025		ZK0803, 86m	greisenization and veinlet-disseminated scheelite on both sides of quartz vein
SM026		ZK0408, 151m	greisenization and veinlet-disseminated scheelite on both sides of quartz vein
SM027		ZK0408, 131m	potash feldspathization, greisenization and veinlet-disseminated scheelite on both sides of quartz vein

 doi:10.20944/preprints202405.0369.v1

SM046	ZK12412, 274m	greisenization and veinlet-disseminated scheelite on both sides of quartz vein
SM047	MZK3608, 96m	greisenization and veinlet-disseminated scheelite on both sides of quartz vein
SM052	MZK2611, 803m	greisenization and veinlet-disseminated scheelite on both sides of quartz vein
SM060	MZK0418, 184m	greisenization and veinlet-disseminated scheelite on both sides of quartz vein
SM061	MZK0418, 265m	greisenization and veinlet-disseminated scheelite on both sides of quartz vein
SM062	KZK0811, 383m	greisenization and veinlet-disseminated scheelite on both sides of quartz vein

Table 2. Homogenization temperatures, salinities, and densities of the fluid inclusions in the Shimensi tungsten deposit.

Sample	Ore body type	t_h/℃	$NaCl_{eq}$ (%)	density(g/cm³)
SM001	thick quartz vein type	169～282	2.90～4.96	0.78～0.93
SM002		155～299	3.55～5.71	0.75～0.95
SM009		174～308	4.03～7.31	0.74～0.95
SM010		170～335	4.49～8.95	0.72～0.94
SM013		161～334	3.55～6.59	0.70～0.95
SM033		193～303	4.80～8.00	0.78～0.93
SM034		198～330	3.55～7.59	0.72～0.92
SM035		190～333	4.96～7.59	0.83～0.93
SM037		153～309	4.65～6.74	0.75～0.96
SM003	hydrothermal crypto-explosive breccia type	139～278	3.06～4.80	0.77～0.96
SM006		168～316	3.55～7.86	0.75～0.95
SM008		168～271	3.23～7.59	0.83～0.94
SM036		191～354	4.96～7.59	0.68～0.92
SM038		147～332	2.58～8.00	0.68～0.94
SM052	veinlet-disseminated type	168～274	2.41～8.68	0.80～0.90
SM056		163～291	4.34～7.59	0.84～0.92
SM060		130～344	3.23～8.68	0.73～0.96
SM061		127～277	2.74～6.59	0.80～0.98
SM021		131～281	5.56～8.14	0.83～0.98
SM062		144～304	4.34～7.17	0.82～0.96
SM024		119～202	2.07～7.59	0.88～0.99
SM025		162～374	4.8～8.68	0.64～0.95
SM026		123～245	4.03～9.47	0.85～0.97
SM027		193～273	5.41～6.45	0.81～0.92
SM046		157～378	2.07～8.81	0.67～0.93
SM047		170～324	4.34～7.45	0.73～0.95

 doi:10.20944/preprints202405.0369.v1

The micro temperature measurement and composition test of inclusions were completed in Beijing Geological Research Institute of China Nuclear Industry. The micro temperature measurement was carried out on the LINKAM THMS600 cold and hot stage, and the working temperature of the cold and hot stage range from196℃~600℃. The test accuracy is ±0.2℃ below 30℃ and ±2℃ above 30℃. According to Campbel and Bodnar et al., the salinity is calculated from the melting temperature and freezing point temperature of the cage [31,32].

The vapor composition of fluid inclusion group is extracted by temperature interval explosion to obtain the fluid vapor composition of different mineralization stages. The Prisma TM QMS200 quadrupole mass spectrometer produced by RG202 in Japan and Anwei in Switzerland was used for the test. The precision of repeated measurement of the instrument is less than 5%[33].

The liquid composition and vapor composition of fluid inclusion group adopt similar means, and the ionic composition of fluid inclusion group in different temperature ranges is extracted by the same temperature range explosion. The ion chromatograph produced by SHIMADZU was used to analyze the relative concentration of ions, and the repeated test accuracy of the instrument was less than 5%. The pretreatment of the extracted ion component sample is the same as that of the vapor component sample.

Laser Raman analysis of single fluid inclusion adopts LABHR-VIS LabRAM HR800 research grade micro laser Raman spectrometer, and the excitation wavelength is: λ=532nm, Yag crystal frequency doubling, solid laser, laser beam spot ≥1μm. The scanning time is 10s with twice scanning.

The samples used for H-O isotope analysis are mainly taken from hydrothermal cryptoexplosive breccia and quartz in quartz vein. Pure quartz shall be selected under the microscope with a purity of more than 99%. The method of oxygen isotope analysis is BrF_5. First, the pure 12mg quartz sample is reacted with BrF_5 for 15h, and the oxygen is extracted. The separated oxygen enters the CO_2 conversion system with a temperature of 700℃ and a time of 12min. Finally, CO_2 is collected. The hydrogen isotope analysis adopts the explosion method to take water from the quartz inclusion. The test procedure is as follows: heat the quartz inclusion sample, make it explode to release volatile matter, extract water vapor, then make the water react with zinc at 400℃ to produce hydrogen, and then freeze it with liquid nitrogen, and collect it into the sample bottle with active carbon. The stable isotope test was completed in the Test Center of Beijing Geological Research Institute of Nuclear Industry with Finningan MAT251EM mass spectrometer. The international standard for hydrogen and oxygen isotopes is V-SMOW, the analysis accuracy of hydrogen isotopes is ±2, and the analysis accuracy of oxygen isotopes is ±0.2.

5. Results

5.1. Distribution and Types of Fluid Inclusions

Microscopic observation shows that there are a large number of fluid inclusions in quartz in different ore bodies of Shimensi tungsten polymetallic deposit. The types of inclusions are diverse, generally distributed in groups or isolated, and a few secondary inclusions are distributed along fractures. The size of inclusions varies greatly, ranging 2×2μm to 20×15μm, but mainly in 6~8 μm. The inclusions are of various shapes, mainly round, oval, strip and irregular.

The objects of this study are all primary inclusions. According to the phase behavior classification criteria of fluid inclusions at room temperature proposed and the phase behavior changes during freezing and rewarming proposed by references [34,35], fluid inclusions can be divided into five types: liquid-rich inclusions(type I), vapor-rich inclusions(type II), pure liquid inclusions(type III), pure vapor inclusions(type IV), fluid inclusions containing a solid crystal(type V).

Type I: liquid-rich inclusion. This type of inclusion is colorless gray, accounting for more than 70% of the total inclusion, and is the main type of fluid inclusion in the ore field. It is mainly round, oval, strip or irregular, composed of vapor and liquids at room temperature, but dominated by liquid. The vapor-liquid ratio is between 10% and 30%, most of which are between 15% and 20%, with a size of 3 to 20μm. Most of them are between 5 and 10μm (Figure 5A and Figure 5B).

 doi:10.20944/preprints202405.0369.v1

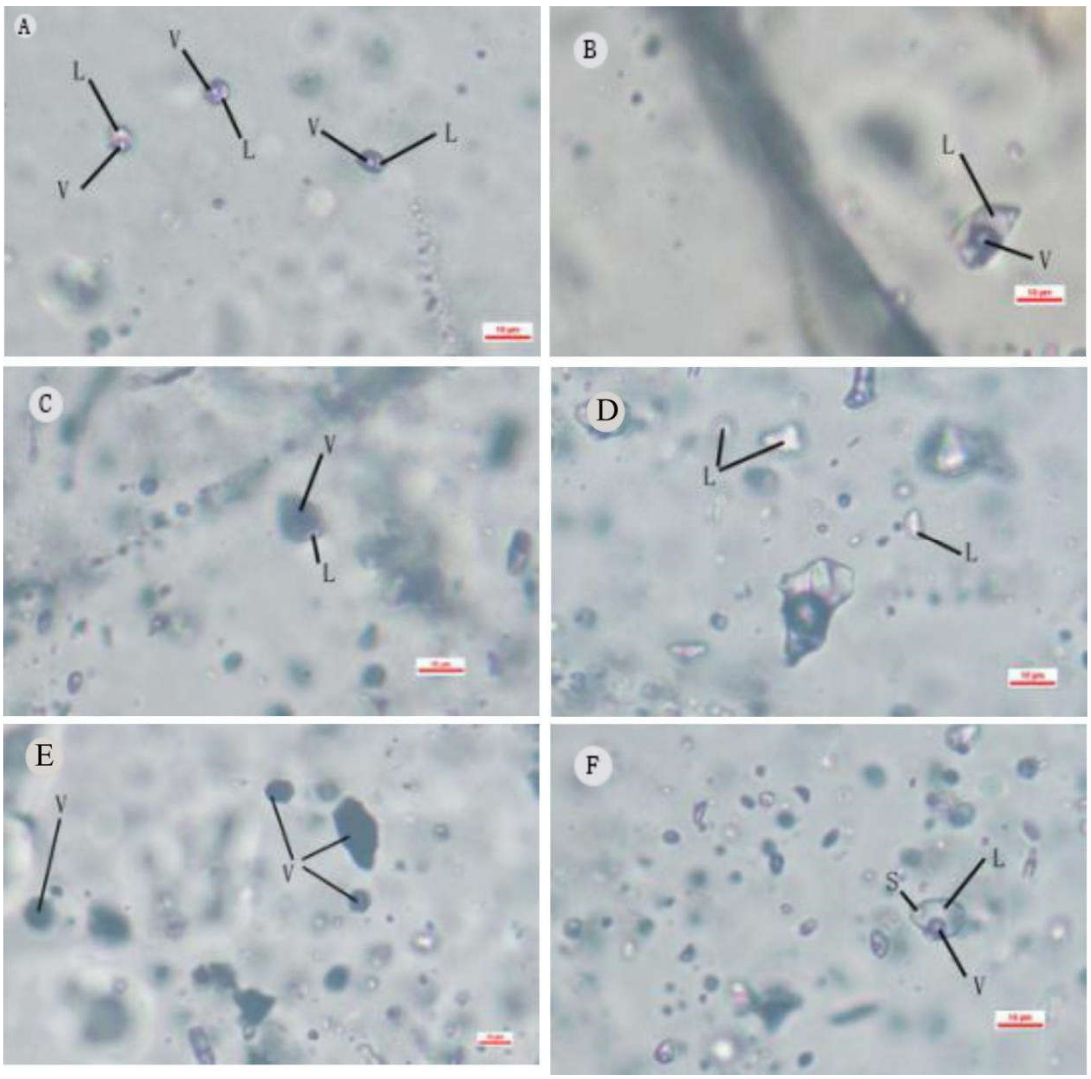

Figure 5. Different types of inclusions in the Shimensi tungsten deposit A and B-liquid-rich inclusions(typeI);C-vapor-rich inclusions(typeII);D-pure liquid inclusions(typeIII); E-pure vapor inclusions(typeIV); F-fluid inclusions containing a solid crystal(typeV) V-vapor; L-liquid; S-solid crystal.

Type II: vapor-rich inclusions: This type of inclusion has a small number, and it is composed of vapor and liquids at room temperature, dominated by vapor. The vapor part accounts for more than 50% of the volume of the entire inclusion, and its filling degree is less than 50%. When the homogenization method is used for temperature measurement on the cold and hot stage, the bubble volume gradually increases with the rising temperature, and finally it turns out to be vapor by adapting the homogenization method. The inclusions are usually round, oval or irregular in shape, occurring in isolation, with a size of 2~10μm. Such inclusions account for about 2% of the total fluid inclusions (Figure 5C).

Type III: pure liquid inclusions. This type of inclusion is less developed, colorless and transparent, mainly round or oval. Only single liquid can be seen at room temperature, and the individual is generally small (2~6μm) , generally distributed in isolation (Figure 5D).

Type IV: pure vapor inclusions. This type of inclusion is small in number, with a vapor volume content of more than 80%. It is dark gray, isolated, usually irregular and long in shape, with a size of 2-15μm (Figure 5E).

Type V: fluid inclusions containing a solid crystal. This type of inclusion is less developed and consists of vapor, liquid and sub minerals. The size of the inclusion is 6-15μm. Generally, it occurs in

 doi:10.20944/preprints202405.0369.v1

isolation, in elliptical or irregular shape, and the minerals are divided into opaque blocks and transparent blocks (Figure 5F).

5.2. Homogenization Temperature, Salinity and Fluid Density

After detailed microscopic observation of primary fluid inclusions in different mineralization stages, the combination type and abundance of fluid inclusions in different stages are determined, and a certain number of representative fluid rich fluid inclusions are measured. The results of micro temperatures measurement show that the rich fluid inclusions of veinlet disseminated ore bodies are developed, and the uniform temperature distribution range is wide, ranging from 119℃ to 378℃, mainly concentrated between 140℃ and 270℃, with an average of 218℃. The salinities are from wt0.88% to wt9.47% NaCl equivalent, concentrated between wt4.03% and wt8.81% NaCl equivalent. The densities of fluid are between 0.64g/cm^3 and 0.99g/cm^3. The homogenization temperatures of hydrothermal cryptoexplosive breccia ore body are 139℃~354℃, mainly concentrated between 170℃~270℃, with an average of 229℃. The salinities are distributed between wt2.57% and wt8.00% NaCl equivalent, concentrated between wt3.06% and wt6.45% NaCl equivalent, and the fluid densities are between 0.68g/cm^3 and 0.96g/cm^3. The homogenization temperatures of quartz vein type ore body are between 153 ℃ and 335℃, mainly between 190℃ and 270℃, with an average of 238℃. The salinities are distributed between wt2.90% and wt8.95% NaCl equivalent, concentrated between wt4.0% and wt7.0% NaCl equivalent, and the fluid densities are between 0.70 g/cm^3 and 0.96 g/cm^3 (Figure 6). Among them, the densities of the inclusions are calculated by the density calculation formula [36].

 doi:10.20944/preprints202405.0369.v1

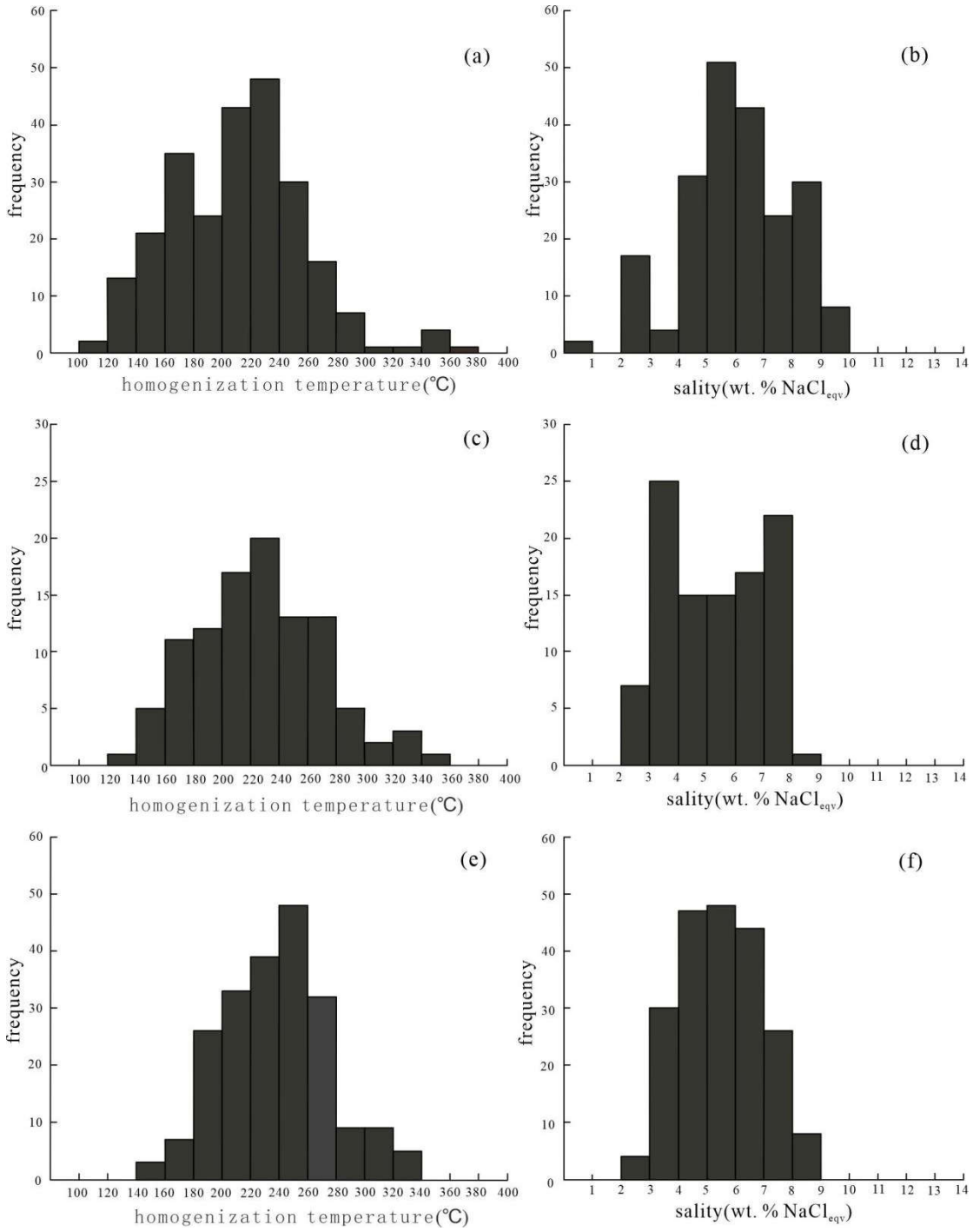

Figure 6. Histograms of homogenization temperature and salinity in different ore type (a)-the homogenezation temperature of the veinlet disseminated orebody; (b)-the salinity of the veinlet disseminated orebody; (c)-the homogenezation temperature of the crypto-explosive breccia orebody; (d)-the salinity of the crypto-explosive breccia orebody; (e)-the homogenezation temperature of the quartz vein type orebody; (f)-the salinity of the quartz vein type orebody.

5.3. Fluid Components

5.3.1. Liquid Composition in Fluid Inclusions

In the liquid composition of fluid inclusions in Shimensi deposit, the anions are mainly SO_4^{2-} (6.443～18.98μg/g), 12.37 μg/g on average, with a small amount of Cl^-（0.7993～1.515μg/g）, NO_3^- (0.1090～0.4108μg/g) and F^-(0.0538～0.3760μg/g). Cations are mainly Na^+ and Ca^{2+}, containing a small

 doi:10.20944/preprints202405.0369.v1

amount of $Mg^{2+}$and K^{+}. Fluid inclusions$(Na^{+}+K^{+})/(Ca^{2+}+Mg^{2+})$ in the area range from 0.407 to 1.246 (0.810 on average). Mg^{2+}/Ca^{2+} ranges from 0.104 to 0.288 (0.179 on average). Na^{+}/K^{+} ranges from 7.551 to 20.834 (13.164 on average). And $SO_4^{2-}/(F^{-}+Cl^{-})$ ranges from 1.074 to 5.617 (3.555 on average).

5.3.2. Vapor Composition in Fluid Inclusions

Convert the unit of vapor composition analysis data of mineral inclusions μg/g ($\omega/10^{-6}$) into its corresponding molar concentration percentage (mol%). It can be seen from the table that the vapor composition in fluid inclusions in Shimensi tungsten polymetallic ore is dominated by H_2O, which has an absolute advantage (the content is more than 99.9mol%) and belongs to high water bearing fluid. In addition, it contains a very small amount of CO_2 (0.00005mol%～0.00057mol%) and trace amounts of N_2, H_2, CO and CH_4.

Table 3. Compositions of the fluid inclusions in Shimensi tungsten deposit.

Sample	F^{-}	Cl^{-}	NO_3^{-}	SO_4^{2-}	Na^{+}	K^{+}	Mg^{2+}	Ca^{2+}	H_2	N_2
SM003	0.3760	1.515	0.4108	6.443	3.169	0.4048	0.7186	4.351	0.00010	0.00016
SM006	0.1871	0.7993	0.2205	8.834	2.814	0.3293	0.5802	6.151	0.00016	0.00010
SM052	0.1131	1.063	0.1537	8.713	1.522	0.3117	0.4103	6.597	0.00116	0.00099
SM026	0.0970	0.9802	0.2301	13.74	2.371	0.5324	0.5865	7.917	0.00059	0.00070
SM001	0.0949	1.258	0.1459	18.98	3.002	0.3498	0.4334	5.608	0.00037	0.00024
SM035	0.0538	1.051	0.1090	17.49	3.471	0.2825	0.6821	3.942	0.00041	0.00016

Sample	CO	CH_4	CO_2	H_2O(vapour)	$(Na^{+}+K^{+})/(Ca^{2+}+Mg^{2+})$	Mg^{2+}/Ca^{2+}	Na^{+}/K^{+}	F^{-}/Cl^{-}	$SO_4^{2-}/(F^{-}+Cl^{-})$	SO_4^{2-}/Cl^{-}
SM003	0.00002	0.00002	0.00021	99.99949	1.068	0.275	13.275	0.464	1.074	1.573
SM006	0.00001	0.00000	0.00005	99.99967	0.735	0.157	14.490	0.437	2.843	4.087
SM052	0.00002	0.00003	0.00022	99.99759	0.407	0.104	8.280	0.199	2.528	3.031
SM026	0.00008	0.00006	0.00057	99.99800	0.525	0.123	7.551	0.185	4.375	5.184
SM001	0.00001	0.00001	0.00015	99.99922	0.881	0.129	14.552	0.141	4.890	5.579
SM035	0.00002	0.00002	0.00021	99.99918	1.246	0.288	20.834	0.096	5.617	6.154

5.4. Laser Raman Spectroscopy Test of Fluid Inclusions

 doi:10.20944/preprints202405.0369.v1

On the basis of micro temperature measurement, the fluid inclusions of quartz in three different types of ore bodies were also analyzed by laser Raman spectroscopy Test. The results show that the composition of inclusions in three different types of ore bodies in the ore district is basically the same. The vapor-liquid inclusions show 2916cm^{-1}, 2329cm^{-1}and 1389cm^{-1} spectral peaks, and the 1285cm^{-1} peak is relatively strong (Figure 7), indicating that there are vapores of CH_4, N_2 and CO_2.

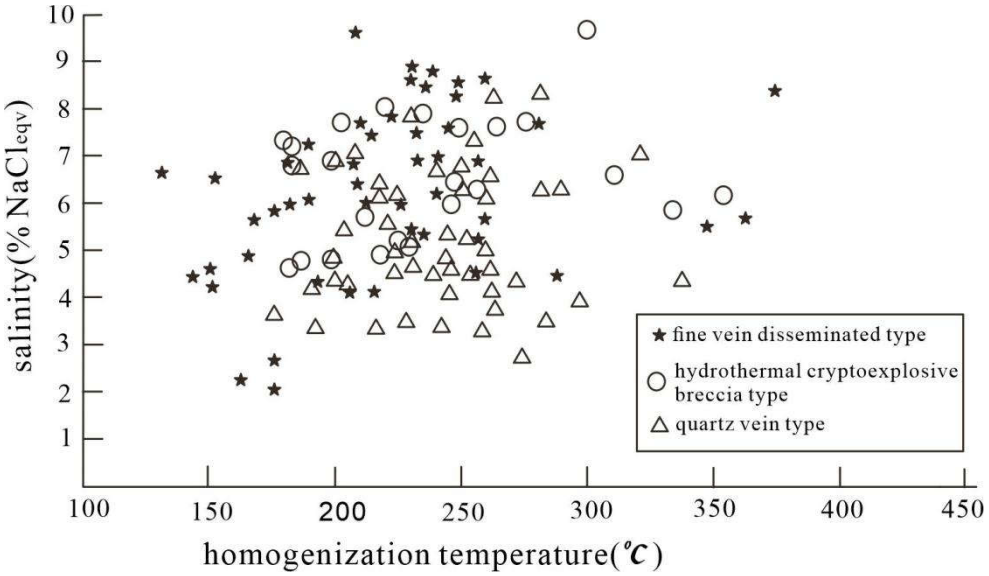

Figure 7. Diagram of the homogenization temperature versus salinity of fluid inclusions in the Shimensi tungsten deposit.

5.5. H-O Isotope Characteristics

The results of hydrogen and oxygen isotope analysis of quartz samples are shown in Table 4. The hydrogen isotope variation of quartz samples is small, ranging from -77.8‰ to -60.6‰, with an average value of -69.25‰. The $\delta D_{V\text{-}SMOW}$ values of hydrothermal cryptoblastic breccia-type ore bodies range from -69.3‰ to -60.6‰, with an average value of -65.79‰. The $\delta D_{V\text{-}SMOW}$ values of quartz vein-type ore bodies range from -77.8‰ to -65‰, with an average value of -71.24‰. The $\delta^{18}O$ values of quartz vary from 12.2‰ to 15.3‰, with an average value of 12.99‰, and the range of variation is small, with a difference of only 3.1‰.

 doi:10.20944/preprints202405.0369.v1

Table 4. Hydrogen and Oxygen isotope compositions of the Shimensi tungsten deposit.

sample	Ore body type	$\delta^{18}O_{quartz}$(‰)	$\delta D_{V\text{-}SMOW}$(‰)	$\delta^{18}O_{H2O}$(‰)	Homogenization temperature (℃)
YQ002	hydrothermal crypto-explosive breccia type	12.6	-67.0	2.02	229
YQ003		12.4	-61.6	1.82	229
YQ006		13.3	-68.6	2.71	229
YQ007		13.5	-60.6	2.91	229
YQ017	veinlet-disseminated type	12.9	-64.2	2.32	229
YQ018		12.5	-69.2	1.92	229
YQ019		13.5	-69.3	2.91	229
YQ020		12.9	-65.0	2.32	229
Q001	thick quartz vein type	12.9	-66.7	2.78	238
Q004		12.9	-74.9	2.78	238
Q005		12.3	-68.7	2.19	238
Q008		15.3	-77.8	5.16	238
Q009		13.2	-68.7	3.08	238
Q010		13.7	-71.7	3.58	238
Q011		12.8	-72.3	2.69	238
Q012		12.2	-70.4	2.09	238
Q013		12.6	-71.7	2.49	238
Q021		12.6	-74.9	2.49	238
Q022		12.7	-72.5	2.59	238

6. Discussion

Most mineralization in the Earth system involves geological fluids, which exert an important influence on the genesis, transport, and precipitation of mineralized materials [35,37]. Therefore, the fluid effects associated with mineralization have attracted many monographs and in-depth studies by scholars. The present experimental results can better reflect the information of mineralizing fluids, so that the mineralizing fluid characteristics, mineralizing pressure range, and mineral precipitation mechanism of Shimenshi tungsten ore can be discussed to restore the mineralizing process.

6.1. Ore-Forming Fluid System

The study of fluid inclusions in the Shimenshi mine area shows that the inclusions are mainly liquid-rich inclusions, with a small number of vapor-rich inclusions, pure liquid inclusions, pure vapor inclusions and fluid inclusions containing a solid crystal, with formation temperatures concentrated in the range of 140°C to 270°C and salinities varying mainly in the range of wt3%-wt5% NaCl equivalent, which are medium to low temperature, low salinity magmatic fluids. The fluid temperature and salinity ranges of the fine-vein dipping, quartz vein type and hidden explosion breccia type ore bodies in the area are basically the same (Figure 7), indicating that the fluids of different mineralization types in the area are the same mineralizing fluid.

The anionic composition of the liquid of the inclusion body indicates that the mineralizing fluid is a hot aqueous solution rich in Na^+, Ca^{2+}, SO_4^{2-}, Cl^- and small amounts of F^- and NO_3^-, which has a strong ability to dissolve mineralized materials. Therefore, the ore-forming fluid of Shimenshi tungsten ore is mainly a Ca^{2+}-Na^+-SO_4^{2-}-Cl^- type fluid.

 doi:10.20944/preprints202405.0369.v1

Mg^{2+} and Ca^{2+} are the most important alkaline metal ions and prevalent elements in hydrothermal fluids, and the Na^{+}/ K^{+} of magmatic hydrothermal fluids is generally less than 1, while the fluids from deeper genesiss contain higher F^{-}, Cl^{-} and larger F^{-}/Cl^{-} [38,39]. The analysis results show that the fluid inclusions have higher Ca^{2+} content, indicating that Ca^{2+} dominates in the mineralizing solution, which is conducive to the formation of scheelite ($CaWO_4$). According to the ion concentration characteristics of the fluid components, the Na^{+}/ K^{+} in the fluid inclusions within the deposit are all greater than 1, while their F^{-}/Cl^{-} are all less than 1. This is mainly due to the characteristics of the mineralizing fluid as a magmatic fluid, and with the mineralization proceeds, atmospheric precipitation enters a larger proportion of the fluid system [20]. The low F^{-} content in fluid inclusions within the Shimenshi mine indicates that F does not play a dominant role in the mineralization process, or it is reduced due to the decrease of atmospheric precipitation.

The vapor in the inclusions is dominated by CO_2 and N_2, and contains a small amount of hydrocarbon vapor components. For the transport mechanism of tungsten in mineralizing fluids, some scholars believe that it may migrate as carbonate and bicarbonate under high temperature conditions [40–42]. However, some others believe that tungsten mainly migrates as multiple complexes [43], and the effect of CO_2 on tungsten in hydrothermal transport is minimal. Although the presence of CO_2 was detected in the fluid composition analysis, its distribution is relatively small, and the mineralization temperature of the deposit is 200°C to 300°C, which is mainly low to medium temperature, and it does not meet the migration conditions of carbonate and bicarbonate under high temperature conditions, indicating that tungsten still mainly migrates as complexes.

6.2. Metallogenetic Process

6.2.1. Ore-Forming Pressure

Inferring the capture pressure based on fluid inclusion thermometry data is one of the important means to restore the original mineralizing environment [44]. The compositional analysis of the mineralizing fluids indicates that the Shimenshi tungsten ore-forming fluid system is the NaCl-H_2O system. For the low and medium salinity systems, the inclusions equivalence equation was used to calculate the mean pressure [36], which ranged from 83.67×10^5Pa to 365.09×10^5Pa for the Shimenshi deposit. The mean pressure of vein disseminated ore body ranges from 150.66×10^5Pa to 365.09×10^5Pa, hydrothermal cryptoexplosive breccia type ore body from 83.67×10^5Pa to 365.09×10^5Pa, quartz vein type ore body from 107.77×10^5Pa to 349.59×10^5Pa. The above three ore bodies show consistent uniform pressure characteristics with a wide range of variation, but the overall pressure values are small and belong to a low-pressure mineralization environment.

This may be caused by two factors. First, as the mineralization works, the mineralization system gradually transforms into an open system, and each mineralization stage contains multiple phases of mineralization fluids, such as the addition of atmospheric precipitation, which leads to a sudden decrease in mineralization pressure. Second, the fluid inclusions in each mineralization stage may be affected by late geological events and the inclusions are damaged, which cannot accurately reflect the mineralization pressure, and the mineralization pressure of some inclusions is lower than 100×10^5Pa, which is obviously inconsistent with the geological phenomenon in the area.

6.2.2. pH Value of Ore-Forming Fluid

pH is a physical quantity that measures the acidity of the mineralizing solution. Generlly it cannot be measured directly from the inclusions, so calculations are made with the help of full analytical data of inclusions composition and chemical equilibrium reactions of mineral coeval combinations. After analysis, the inclusions in the Shimenshi mine turn out to belong to the low-salinity NaCl-H_2O fluid system, so the concentration approximation can be used instead of activity in the calculation. In addition to the H_2O and NaCl components, five main ions are present in the NaCl-H_2O hydrothermal fluid: H^{+}, OH^{-}, HCl, Cl^{-}, and Na^{+}, and the total mass balance is reached. Based on the calculating formula by Liu et al.[36], it can be concluded that the pH value of

 doi:10.20944/preprints202405.0369.v1

mineralizing fluids in the Shimenshi ore district ranges from 5.14 to 5.34 in the corresponding temperature-pressure range. The pH values of the mineralizing fluids do not vary much in each stage and all show a weakly acidic mineralizing condition, which is basically consistent with the mineralizing fluids in regional porphyry tungsten ores [45].

6.2.3. Eh Value of Ore-Forming Fluid

Eh value represents the oxidation-reduction potential of mineralizing solution, which can quantitatively measure the degree of oxidation-reduction of mineralizing solution. The Eh value of the mineralizing fluid is closely related to the pH value of the solution, and its calculation is based on the vapor-liquid equilibrium relationship of fluid inclusions, where the equilibrium vapor compositions include CH_4(g), CO_2(g), and H_2O(g), and the equilibrium liquid is mainly H_2O(l). -0.08 between. It can be seen that the Eh values of its fluids do not vary much, showing a weakly reducing environment.

6.3. Genesis of Ore-Forming Fluid

The hydrogen isotope variation of the quartz samples is small, with an average value of -71.24‰, all in the range of normal magmatic water (-80‰ to -50‰)[46], indicating that the original fluid of the mineralizing fluid came from the magma itself. The $\delta^{18}O$ value of quartz varies between 12.2‰ and 15.3‰, with an average value of 12.99‰, showing the granitic $\delta^{18}O$ (7‰-13‰) characteristics [47]. With reference to the measured fluid inclusion homogeneous temperatures of hydrothermal cryptogenic breccia-type ore bodies and quartz vein-type ore bodies in the Shimensi tungsten polymetallic deposit, the $\delta^{18}O$ water values of hydrothermal water in equilibrium with quartz in both ore body types were calculated using the quartz-water fractionation equation at 229°C and 238°C. By virtue of $\delta^{18}O$ values of quartz and the homogeneous temperatures of minerals [48], the calculated $\delta^{18}O$ values of the mineralized fluids vary between 1.82‰ and 5.16‰, with an average value of 2.68‰. The $\delta^{18}O$ values of mineralizing fluids in hydrothermal cryptoblastic breccia ore bodies vary from 1.82‰ to 2.91‰, with an average value of 2.37‰. The $\delta^{18}O$ values of mineralizing fluids in quartz vein ore bodies vary from 2.19‰ to 5.16‰, with an average value of 2.90‰, all deviating from the range of magmatic water variation. In the δD-$\delta^{18}O_{H2O}$ water diagram (Figure 10), the sample points fall below and to the left of the magma water, i.e., the transition area between magma water and atmospheric precipitation.

 doi:10.20944/preprints202405.0369.v1

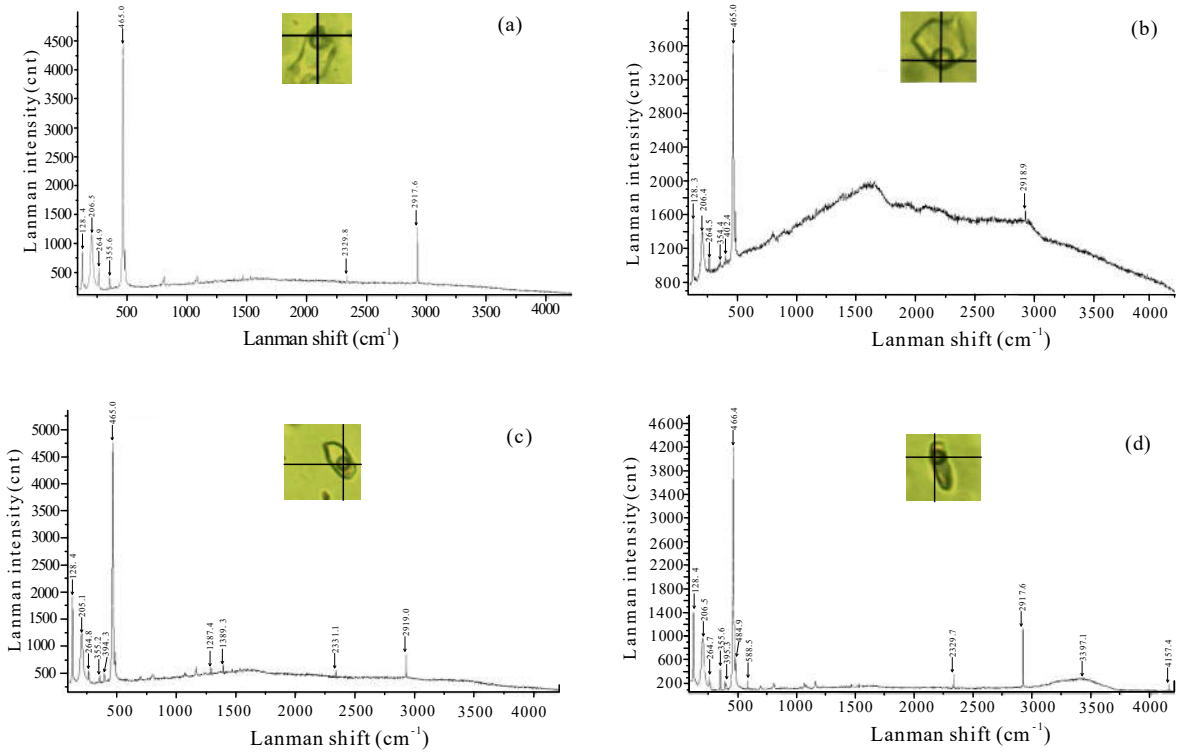

Figure 8. Laser Laman spectra of fluid inclusions in the Shimensi tungsten deposit.

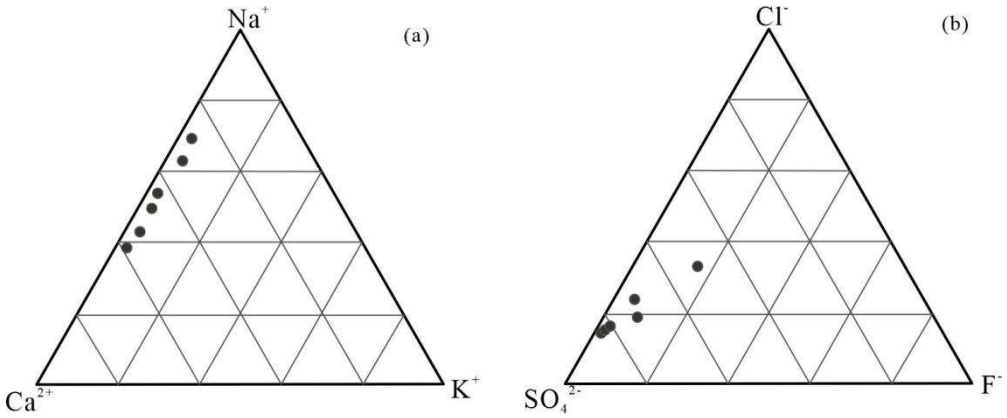

Figure 9. The trigonometry of the liquid phase composition of the fluid inclusions in the Shimensi tungsten deposit.

 doi:10.20944/preprints202405.0369.v1

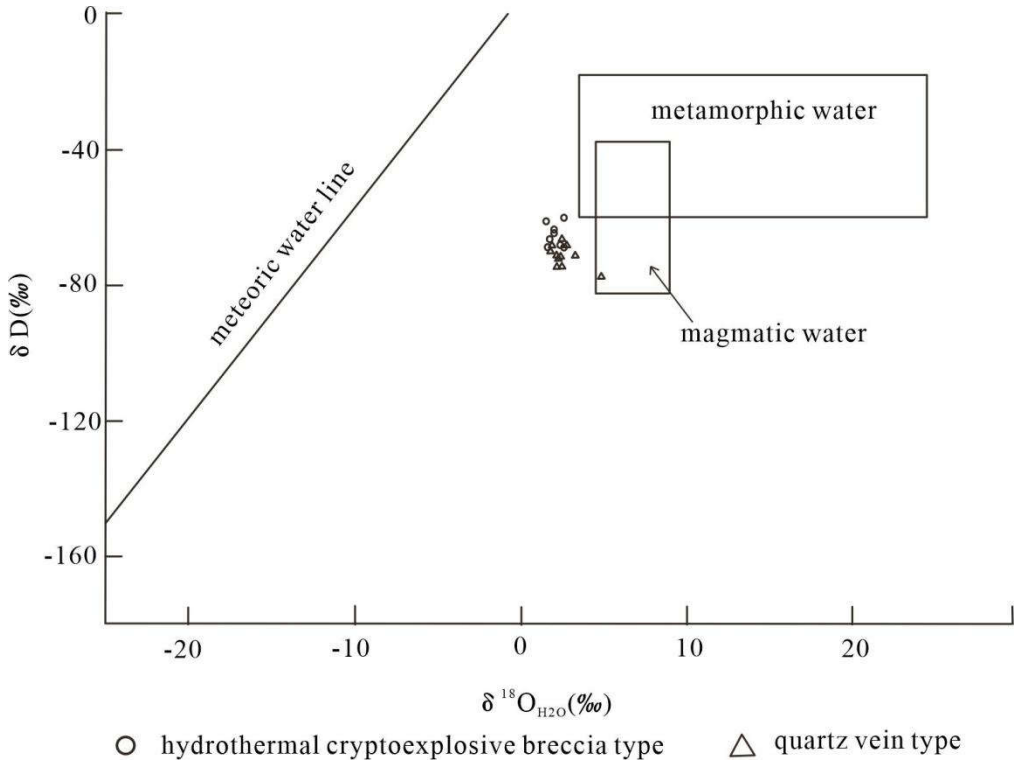

Figure 10. $\delta D_{V\text{-}SMOW}$-$\delta^{18}O_{H2O}$ diagram of fluid inclusions in the Shimensi tungsten deposit.

It has been shown that many factors can influence the hydrogen and oxygen isotopic compositions of mineralized fluids, such as mineralization temperature, type of water, W/R ratio during water-rock exchange, etc. The lack of hydrogen and oxygen isotope values for the surrounding rocks and the Yanshan-age atmospheric precipitation makes it difficult to explore the specific water-rock reaction patterns in the mine area. However, quartz is prone to undergo isotope equilibrium re-exchange reactions with the water it contains, causing the measured oxygen isotopic compositions of the inclusions to not fully reflect the $\delta^{18}O_{H2O}$ water values of the original ore-bearing solution. But quartz contains almost no hydrogen atoms, so the exchange effect on the hydrogen isotopic compositions of the fluid inclusions is minimal [49]. The surrounding rocks of the mine are biotite granodiorite, which also contains hydrogen-bearing minerals, but if the water-rock exchange reaction occurs, the hydrogen isotopic composition of the fluid will not change greatly after the exchange, i.e., this change is negligible [50]. Therefore, the hydrogen isotopic composition represents the composition of the original solution. δD-$\delta^{18}O_{H2O}$ water values deviate from the normal magma water values, giving rise to an obvious "oxygen drift". The reason for this phenomenon may be the addition of atmospheric precipitation, which caused the drift of oxygen isotopes to atmospheric precipitation.

The H and O isotopic compositions of the Shimenshi tungsten polymetallic deposit are mainly derived from magmatic fluids that were mixed with atmospheric precipitation during and evolved, which is consistent with most current studies on the genesis of mineralizing fluids for tungsten deposits [7,42,50].

6.4. Mineral Precipitation Mechanism

Previous studies have shown that miscibility of fluids, cooling of the fluid system, boiling of the fluid system, and reduction of fluid pressure are important mechanisms for tungsten precipitation in fluids [40,51–55].

The mineralizing fluids of tungsten deposits are considered by previous authors to be mainly magmatic water with the mixing of atmospheric precipitation. In this paper, the results of H and O isotope analysis indicate that the mineralizing fluid of Shimenshi tungsten deposit is mainly derived

 doi:10.20944/preprints202405.0369.v1

from magmatic hydrothermal fluid with the mixing of atmospheric precipitation during the evolution. Therefore, the mixing of different fluids is the main factor of the precipitation of tungsten ore.

In general, boiling of fluids will result in a series of inclusions capturing different liquid and vapor ratios. The mineralizing fluids are apparently multicomponent fluids, in addition to the main equisolutes, the fluid also contains trace equicomponents, often in close symbiosis, showing that they are captured in an inhomogeneous fluid state [56]. This phenomenon may be caused by single fluid immiscibility. The petrographic study of fluid inclusions shows that the proportion of "fluid boiling" phenomenon, where liquid-rich inclusions coexist with vapor-rich inclusions and pure vapor inclusions, is low at Shimenshi tungsten mine. This indicates that overall, this phenomenon contributes little to mineralization. Therefore boiling is not a major factor in the precipitation of tungsten ore.

Sudden changes in pressure usually lead to boiling, accompanied by changes in fluid inclusion volume and density [57]. Fluid inclusion tests show a wide range of pressure variation in the Shimensi mine, but the whole may have been damaged at a later stage and does not reflect the mineralization process. Petrographic observations of fluid inclusions in the area did not reveal significant changes in inclusions volume, and density variations range from 0.64 g/cm^3 to 0.99 g/cm^3, indicating that pressure reduction is not the main mechanism leading to mineral precipitation.

Also, the cooling effect of the fluid system is one of the main mechanisms of tungsten precipitation in fluids [51,58–60]. It was shown that the solubility of wolframite, scheelite, and other tungsten minerals in the fluids increased significantly when the temperature increased [43], which shows that the effect of temperature change on tungsten precipitation is obvious. The present study shows that fluid inclusion thermometry data in the mine area show a wide range of mineralization temperature variation (119°C to 378°C). Salinity decreases with falling homogeneous temperature. The three different types of ore bodies have common variation characteristics, so the decrease of temperature may also play a role in promoting the precipitation enrichment of the mineral matter in is Shimenji ore district.

7. Conclusions

(1) The fluid inclusions of quartz in the Shimenshi tungsten polymetallic deposit are classified into five types, including liquid-rich inclusions (type I), pure liquid inclusions (type II), vapor-rich inclusions (type III), pure vapor inclusions (type IV), and fluid inclusions containing a solid crystal (type V). Microcalorimetry results show that the homogeneous temperature distribution of fluid inclusions in each mineralization stage is wide, ranging from 119°C to 378°C. The salinities variey from wt0.88% to wt9.47% NaCl equivalent, and the densities of the fluid are between 0.64 g/cm^3 and 0.99 g/cm^3, which belong to low-density fluid.

(2) The liquid anion and cation components of fluid inclusions in the region are rich in Na^+, Ca^{2+}, SO_4^{2-}, Cl^- and a small amount of F^- and NO_3^-. The vapor components are mainly H_2O, which belong to NaCl-H_2O fluid system containing a small amount of CO_2, CH_4 and N_2. The high Ca^{2+} content in the fluid inclusions is favorable to the formation of scheelite（$CaWO_4$）.

(3) The mineralization pressure pressure of the Shimensi deposit ranges from 83.67×10^{5}Pa to 365.09×10^{5}Pa. The mean pressure of the fine-vein dipping type ore body ranges from 150.66×10^{5}Pa to 365.09×10^{5}Pa, the hydrothermal cryptoblastic breccia type ore body from 83.67×10^{5}Pa to 221.67×10^{5}Pa, the quartz vein type ore body from 107.77×10^{5}Pa to 349.59×10^{5}Pa. The variation ranges widely, but the overall pressure value is small, which refers to a low-pressure metallogenic environment. The pH values in the corresponding temperature-pressure range are 5.14 to 5.34, indicating a weakly acidic metallogenic condition, which is basically consistent with the metallogenic fluid of regional porphyry tungsten ore. The Eh values are between -0.14 and -0.08, showing a weakly reducing environment.

(5) The H-O isotope test results show that the $\delta D_{V\text{-}SMOW}$ values of the quartz samples range from -77.8‰ to -60.6‰, and the average $\delta^{18}O$ value of the mineralizing fluid is 2.90‰, indicating that the mineralizing fluid of the Shimenshi tungsten polymetallic deposit mainly originates from the magma and has the mixing effect of atmospheric precipitation during the ascending process. The lower

temperature may play a certain role in the precipitation enrichment of tungsten elements. The lower temperature may have contributed to the precipitation enrichment of tungsten.

Acknowledgments: This research is jointly funded by the Mineral Geology of China Geological Survey (DD20190379, DD20160346), the Natural Science Basic Research Program of Shaanxi Science and Technology Department, China (2023-JC-QN-0286), the State-owned Capital Management Budget Fund Project of Shaanxi Province,China(2023-), the GSFC program(Grant No.41962012)..Conferences.

Reference

1. Li, Y.D.; Sheng, J.F.; Bel, L.L.; Giuliani, G. Evidengce for the lower continental crustal origin of the Xihuashan granite. *Acta Geoleogca Sinica (English Edition)*. 1986,60,47-64.
2. Wei, W.F.; Hu, R.Z.; Peng, J.T.; Bi, X.W.; Song, S.Q.; Shi,S.H. Infrared microthermometric and stable isotopic study of fluid inclusions in wolframite at the Xihuashan tungsten deposit, Jiangxi province, China. *Mineralium deposita*. 2012,47,589-605.
3. Yang,J.H.; Peng,J.T.; Zhao, J.H.; Fu,Y.Z.;Yang, C.; Hu,Y.L. Petrogenesis of the Xihuashan Granite in Southern Jiangxi Province,South China: Constraints from Zircon U-Pb Geochronology, Geochemistry and Nd Isotopes.*Acta Geoleogca Sinica (English Edition).* 2012,86,131-152.
4. Liu, X.C.; Xing,H.L.; Zhang, D.H.Fluid focusing and its link to vertical morphological zonation at the Dajishan vein-type tungsten deposit, South China. *Ore Geology Reviews*. 2014,62,245-258.
5. Mao, Z.H.; Cheng, Y.B.; Liu, J.J.; Yuan, S.D.; Wu, S.H.; Xiang, X.K.; Luo, X.H. Geology and molybdenite Re-Os age of the Dahutang granite-related veinlets-disseminated tungsten ore field in the Jiangxi Province, China. *Ore Geol. Rev.* 2013,53,422-433.
6. Mao, J.W.; Yuan, S.D.; Xie, G.Q, Song, S.W.; Zhou Q.; Gao, Y.B.; Liu, X.; Fu, X.F.; Cao, J.; Zeng, Z.L.; Li T.G.; Fan X.Y. New advances on metallogenic studies and exploration on critical minerals of China in 21st century. *Mineral Deopsits*. 2019,38,935-969(in Chinese with English abstract).
7. Feng, C.Y.; Zhang, D.Q.; Xiang, X.K.; Li, D.X.; Qu, H.Y; Liu, J.N.; Xiao, Y. Re-Os isotopic dating of molybdenite from the Dahutang tungsten deposit in northwestern Jiangxi Province and its geological implication. *Acta Petrol. Sin.* 2012,28(12):3858-3868 (in Chinese with English abstract).
8. Sun, K.K.; Chen, B. Trace elements and Sr-Nd isotopes of scheelite: Implications for the W-Cu-Mo polymetallic mineralization of the Shimensi deposit, South China. *American Mineralogist*. 2017,102:1114-1128.
9. Xiang, X.K.; Chen, M.S. Zhan, G.N.; Qian, Z.Y.; Li, H.;Xu, J.H. Metallogenic geological conditions of Shimensi tungsten-polymetallic deposit in North Jiangxi Province. Contributions to Geology and Mineral Resources Research. 2012,27,143-155(in Chinese with English abstract).
10. Xiang, X.K.; Wang, P.; Zhan, G.N.; Sun, D.M.; Zhong, B.; Qian, Z.Y.; Tan, R. Geological characteristics of Shimensi tungsten polymetallic deposit in Northern Jiangxi province. *Miner. Depos*. 2013,32,1171-1187 (in Chinese with English abstract).
11. Feng, C.Y.; Wang, S.; Zeng, Z.L.; Zhang, D.Q.; Li, D.X.; She, H.Q.;. Fluid inclusion and chronology studies of Baxiannao mineralized fractured zone-type tungsten polymetallic deposit, southern Jiangxi province, China. *Acta Petrol. Sin*. 2012,28,52-64 (in Chinese with English abstract).
12. Huang, L.C.; Jiang, S.Y. Zircon U-Pb geochronology, geochemistry and petrogenesis of the porphyric-like muscovite granite in the Dahutang tungsten deposit, Jiangxi Province. *Acta Petrol. Sin*. 2012,28,3887-3900 (in Chinese with English abstract).
13. Huang, L.C.; Jiang, S.Y. Geochronology, geochemistry and petrogenesis of the tungsten-bearing porphyritic granite in the Dahutang tungsten deposit, Jiangxi Province. *Acta Petrol. Sin*. 2013,29,4323-4335 (in Chinese with English abstract).
14. Huang, L.C.; Jiang, S.Y. Highly fractionated S-type granites from the giant Dahutang tungsten deposit in Jiangnan Orogen, Southeast China: geochronology, petrogenesis and their relationship with W-mineralization. *Lithos*. 2014,202-203,207-226.
15. Mao, Z.H.; Liu, J.J.; Mao, J.W.; Deng, J.; Zhang, F.; Meng, X.Y.; Xiong, B.K.; Xiang, X.K.; Luo, X.D. Geochronology and geochemistry of granitoids related to the giant Dahutang tungsten deposit, middle Yangtze River region, China: Implications for petrogenesis, geodynamic setting, and mineralization. *Gondwana Res*. 2014,7,1-21.
16. Xiang, X.K.; Chen, M.S.; Zhan, G.N.; Qian, Z.Y.; Li, H.; Xu, J.H. Metallogenic geological conditions of Shimeisi tungsten-polymetallic deposit in north Jiangxi Province. *Contrib. Geol. Miner. Resour. Res*. 2012,27,143-155 (in Chinese with English abstract).
17. Xiang, X.K.; Liu, X.M.; Zhan, G.N. Discovery of Shimensi super-large tungsten deposit and its prospecting significance in Dahutang area, Jiangxi Province. *Resour. Suvey Environ*. 2012, 33,141-151 (in Chinese with English abstract).

18. Xiang, X.K.; Wang, P.; Sun, D.M.; Zhong, B. Isotopic Geochemical characteristics of the Shimensi tungsten-polymetallic deposit in northern Jiangxi Province. *Acta Geosci. Sin*. 2013,34,263-271 (in Chinese with English abstract).
19. Xiang, X.K.; Wang, P.; Zhan, G.N.; Sun, D.M.; Zhong, B.; Qian, Z.Y.; Tan, R. Geological characteristics of Shimensi tungsten polymetallic deposit in Northern Jiangxi province. *Miner. Depos*. 2013,32,1171-1187 (in Chinese with English abstract).
20. Gong, X.D.; Yan, G.S.; Ye, T.Z.; Zhu, X.Y.; Li, Y.S.; Zhang, Z.H.; Jia, W.B.; Yao, X.F. A study of ore-forming fluids in the Shimensi tungsten deposit, Dahutang tungsten polymetallic ore field, Jiangxi Province, China. *Acta Geol. Sin*. 2015, 89,822-835 (English Edition).
21. Ye, Z.H.; Wang, P.; Xiang, X.K.; Yan, Q.; Li, Y.K.; Guo, J.H. Early Cretaceous tungsten mineralization in Southeastern China: the Wuning example. *Inter Geol. Rev*. 2016,59,946-964.
22. Wei, W.F.; Lai, C.K.; Yan, B.; Zhu, X.; Song, S.; Liu, L. Petrogenesis and metallogenic implications of Neoproterozoic granodiorite in the super-large Shimensi tungsten-copper deposit in northern Jiangxi, South China. *Minerals*. 2018,8,1–22.
23. Wei, W.F.; Shen, N.P.; Yan, B.; Lai, C.K.; Yang, J.H.; Gao, W.; Liang, F. Petrogenesis of ore-forming granites with implications for W-mineralization in the super-large Shimensi tungsten-dominated polymetallic deposit in northern Jiangxi Province, South China. *Ore Geol. Rev.* 2018,95,1123–1139.
24. Wang, P. Geology, Fluid inclusion, Stable isotope and molybdenite Re-Os Constraints on the Genesis of the Shimensi Tungsten Metallogenic deposit, Northern Jiangxi Province: Tianjin. *Sinosteel Tianjin Geological Academy*. 2013,1-85 (in Chinese with English abstract).
25. Wang, P.; Liang, T.; Jiang, H.; Xiang, X.; Zhong, B. Trace Elements and Pb-O Isotopes of Scheelite: Metallogenic Implications for the Shimensi W-Polymetallic Deposit in South China. *Minerals*. 2022,12,1461.
26. Shu, L.S. An analysis of principal features of tectonic evolution in South China Block. *Geological Bulletin of China*. 2012,31,1035-1053(in Chinese with English abstract).
27. Wang, X.L.; Zhou, J.C.; Chen, X.; Zhang, F.F.; Sun, Z.M. Formation and evolution of the Jiangnan orogen. *Bulletin of Mineralogy, Petrology and Geochemistry*. 2017,36,714-735+696 (in Chinese with English abstract).
28. Zhao, Z.; Liu, C.; Guo, N.X.; Zhao, W.W.; Wang, P.A.;Chen, Z.H. Temporl and spatial relationships of granitic magmatism and W mineralization: Insights from the Xingguo orefield, South China. *Ore Geology Reviews*.2018,95,945-973.
29. Chang, Y.F.; Li, J.H.; Song C.Z. The regional tectionic framework and some new understandings of the Middle Lower Yangtze River Valley Metallogenic Belt. *Acta Petrologica Sinica*. 2019,35,3579-3591(in Chinese with English abstract).
30. Xiang, X.K.; Wang, S.L.; Zhan, G.N.; Xiao, E.; Hu, A.N.; Hu, B.Z.; Pan, W.J. Geological Feature of "one area three ore types"of a W -Cu-Mo deposit in Shimei Temple Area. *The Ninth Geological Science and Technology Forum in East China, Hangzhou, Zhejiang Province*.2011,60-71(in Chinese with English abstract).
31. Campbell, A.R.; Panter, K.S. Comparison of fluid inclusions in coexisting (cogenetic?) wolframite, cassiterite, and quartz from St. Michael's Mount and Cligga Head, Cornwall, England. *Geochimica et Cosmochimica Acta.* 1990,54,673–681
32. Bodnar, R. J.;Vityk, M.O. Interpretation of microthermetric data for H_2O-NaCl fluid inclusions. In fluid inclusions in minerals: Methods and Applications(eds. B.De Vivo and M.L.Frezzotti). Virginia Tech, Blacksburg,1994,117-130.
33. Zhu, H.P.; Wang, L.J.; Liu, J.M. Determination of quadrupole mass spectrometer for gaseous composition of fluid inclusion from different mineralization stages. *Acta Petrologica Sinica*.2003,19,314-318.
34. Roedder, E. Fluid inclusions. Mineralogical Society of America,Reviews in Mineralogy. 1984.,12,25-35.P.273.
35. Lu, H.Z.; Fan, H.R.;, NI, P.; Ou G.X.; Shen, K.; Zhang W.H. Fluid inclusions(First Edition). *Beijing: Science and Technology Press*.2004,pp.406-419(in Chinese)
36. Liu, B.; Shen, K. Fluid inclusion thermodynamics. *Beijing,Geological Publishing House*. 1999, pp.207-208(in Chinese).
37. Zhu, H.L.; Zhang, L.P.; Du, L.; Sui, Q.L. The geochemical behavior of tungsten and the genesis of tungsetn deposit in South China. *Acta Geoscientica Sinica*. 2020,36,13-22(in Chinese with English abstract).
38. Lu, H.Z. The origin of tungsten mineral deposits in south China. *Chongqing: Chongqing Publishing House*.1986,pp.1-230(in Chinese).
39. Feng, C.H.; Wang S.; Zeng, Z.L.; Zhang, D.Q.; Li, D.X.; She, H.Q. Fluid inclusions and chronology studies of Baxiannao mineralized fractured zone-type tungsten polymetallic deposit , south Jiangxi Province, China. Acta Petrologica Sinica, 2012,28, 52-64(in Chinese with English abstract).
40. Higgins, N.C.; Kerrich R. Progressive ^{18}O depletion during CO_2 separation from a carbon diocide-rich hydrothermal fluid：Evidence from the Grey River tungsten deposit， *Newfoundland. Can. J. Earth. Sci.* 1982, 19,2247-2257.

41. Rios,F. J.; Villas, R.N.; Fuzikawa, K. Fluid evolution in the Pedra Preta wolframite ore deposit. Paleoproterozic Musa Granite, East Amazon Craton, Brazil. *Journal of South American Earth Sciences.* 2003,15,787-802.
42. Wang, X.D.; Ni, P.; Jiang, S.Y.; Zhao, K.D.; Wang, T.G. Origin of the ore-forming fluid in the Piaotang tungsten deposit in Jiangxi Province:Evidence from helium and argon isotope. Chinese Science Bull. 2010,55,3338-3344.
43. Wood,S.A.; Samson,I.M. The hydrothermal geochemistry of tungsten in granitoid environments: Ⅰ. Relative solubilities of ferberite and scheelite as a function of T, P, pH, and mNaCl. Economic Geology. 2000,95,143-182.
44. Roedder, E.; Bodnar, R.J. Geologic Pressure Determinations from Fluid Inclusion Studies. Annual Review of Earth and Planetary Sciences. 1980,8,263-301.
45. Tan, Y.J. The metallogenic mechanism of the Lianhuashan porphyry tungsten deposit. Science China (B). 1985, 6,563-570.
46. Zheng, Y.F.; Chen,J.F. Stable isotope geochemistry. Beijing, Science Press.2000, pp.243-245(in Chinese).
47. Zhang, Z.X.; Yang, F.Q.; Yan, S.H.; Zhang,R.;Chai, F.M.; Liu, F.M.; Geng, X.X. Sources of ore-forming fluid and materials of the Baogutu porphyry copper deposit in Xinjiang Constraints from sulpher-hydrogen-oxygen isotopes geochemistry. Acta Petrologica Sinica. 2010,26,707-716 (in Chinese with English abstract).
48. Clayton, R.N.; O'Neil, J.R.; Mayeda, T.K.Oxygen isotope exchange between quartz and water. Journal of Geophysical Rearch. 1972,77,3057-3067.
49. Ding, T.P.; Liu, Y.S.; Wan, D.F.; Liu, Z.J.; Li, J.C.; Zhang, G.L. Study on quartz-tungsten iron ore oxygen isotope geothermometer and its geological application. Acta Geologica Sinica. 1992,66,48-58(in Chinese)
50. Song, S.Q.; Hu, R.Z.; Bi, X.W.; Wei, W.F.; Shi, S.H. Fluid inclusions geochemistry of the Taoxikeng tungsten deposit in southern Jiangxi Province, China. Geochemica, 2011,40,237-248.
51. Seal, R.R.; Clark, A.H.; Morrissey, C.J. Stockwork tungsten (scheelite)-molybdenum mineralization, Lake George, Southwestern New Brunswick. Econ. Geol. 1987,82,1259-1282.
52. Lynch, J.V. Hydrothermal alteration, veining, and fluid inclusion characteristics of the Kalzas wolframite deposit, Yukon. Can. J. Earth. Sci.1989,26,2106-2115.
53. Polya,D.A. Chemistry of the main-stage ore-forming fluids of the Panasqueira W-Cu(Ag)-Sn deposit. Portugal： Implications for models of ore genisis. Econ. Geol.1989,84,1134-1152.
54. Giamello, M.; Protano, G.; Riccobono,F, Sabatini, G. The W-Mo deposit of Perda Majori (SE Sardinia, Italy): A fluid inclusion study of ore and gangue minerals. Eur. J. Mineral. 1992,4,1079-1084.
55. So, C.S.; Yun, S.T. Origin and evolution of W-Mo-producing fluids in a granitic hydrothermal system：Geochemical studies of quartz vein deposits around the Susan granite, Hwanggangri district, Republic of Korea. Econ. Geol.1994,89,246-267.
56. Shepherd, T.J.; Rakin, A.; Alderton. D.H.M. A Practical Guide to Fluid Inclusion Studies. Black and Son Limited. 1985,pp.1-154.
57. Zezin, D.Y.; Migdisco, A.A.; Williams, A.E. The solubility of gold in H_2O-H_2S vapor at elevated temperature and press. Geochemica et Cosmochimica Acta. 2011,75,5140-5153.
58. Ramboz, C.; Schnapper, D.; Dubessy, J. The P-V-T-X-f_{O2} evolution of H_2O-CO_2-CH_4 bearing fluids in a wolframite vein: Reconstruction from fluid liclusion studies. Geochem. Cosmochim. Acta. 1985,49,205-219.
59. Samson, I.M. Fluid evolution and mineralization in a subvolcanic granite stock： The Mount Pleasant W-Mo-Sn deposits,New Brunswick, Canada. Econ. Geol.1990,85,145-163.
60. O'Reilly,C; Gallagher, V.; Feely, M. Fluid inclusion study of the Ballinglen W-Sn-sulphide mineralization, SE Ireland. Mineralium Deposita.1997,32,569-580.